Association between oropharyngeal microbiome and weight gain in piglets during pre and post weaning life

Andrew Wange Bugenyi[1], Ho-Seong Cho[2] and Jaeyoung Heo[3]*

[1]Department of Agricultural Convergence Technology, Jeonbuk National University, Jeonju 54896, Korea
[2]College of Veterinary Medicine and Veterinary Diagnostic Center, Jeonbuk National University, Iksan 54596, Korea
[3]International Agricultural Development and Cooperation Center, Jeonbuk National University, Jeonju 54896, Korea

*Corresponding author
Jaeyoung Heo
International Agricultural Development
and Cooperation Center,
Jeonbuk National University,
Jeonju 54896, Korea.
Tel: +82-63-270-5926
E-mail: jyheobio@gmail.com

ORCID
Andrew Wange Bugenyi
https://orcid.org/0000-0001-9036-8391
Ho-Seong Cho
https://orcid.org/0000-0001-7443-167X
Jaeyoung Heo
https://orcid.org/0000-0002-9721-8043

Abstract

Birth weight and subsequent weight gain is of critical importance in the survival and performance of piglets on a commercial swine farm setting. Oropharyngeal microbiome could influence immunity, and feeding behavior thus impacting health and weight gain. We used 16S rRNA gene sequencing to profile the composition and predicted metabolic functionality of the oropharyngeal microbiota in 8 piglets (4 with a birthweight ≤ 1.0 kg and 4 with a birthweight ≥ 1.7 kg) at 11, 26, and 63 days of age. We found 9 genera that were significantly associated with average daily gain (ADG) at 11 days (false discovery rate, FDR < 0.05) and 26 days of age (FDR < 0.1), respectively. The microbial functional profile revealed several pathways associated with ADG (FDR < 0.05). Among these, pathways related to degradation of catechols showed a positive association with ADG at 11, 26, and 63 days of age, implying a potential to breakdown the host-derived catecholamines. We also noted that pathways related to the biodegradation of nucleosides and nucleotides increased with ADG during the pre-weaning phase, while those involved in their biosynthesis decreased. Our findings provide insights into the oropharyngeal microbial memberships and metabolic pathways that are involved in a piglet's weight gain. Thus, providing a basis for the development of strategies aimed at improving weight gain in pigs.

Keywords: Swine, Oropharyngeal, Microbiome, Birthweight, Average daily gain

INTRODUCTION

Low-birthweight piglets are associated with a reduced survivability and performance [1], thus contributing to the high production costs encountered by many commercial swine enterprises. Most of the management interventions to alleviate these impacts, have been based on optimizing intake of nutritious feed and use of growth promoters, including antibiotics [2]. However, these methods have yielded mixed results. Further, the use of antibiotics could have short- and long-term effects on the health of the animals as well as contribute to the propagation of antimicrobial resistance [3,4].

Meanwhile, recent studies have shown that the microbial composition along the digestive tract has a considerable bearing on the development of the host's immune system [5] and efficiency of nutrient

Authors' contributions
Conceptualization: Bugenyi AW, Heo J.
Data curation: Bugenyi AW.
Formal analysis: Bugenyi AW, Cho HS.
Methodology: Bugenyi AW, Cho HS, Heo J.
Software: Bugenyi AW, Cho HS.
Validation: Bugenyi AW, Heo J.
Investigation: Bugenyi AW, Heo J.
Writing - original draft: Bugenyi AW.
Writing - review & editing: Bugenyi AW, Heo J.

utilization [6] thus potentially promoting survival and weight gain. Other areas where the microbiota has been found to play important roles include drug metabolism [7] and feeding behavior [8] further affecting health and weight gain, respectively. However, the microbiota is simple and unstable in piglets and has to mature into a relatively more complex and stable community in order to optimally confer these benefits to the animal. Around the time of birth, the neonate receives microbial inocula from its interaction with the sow and the immediate environment [9]. This interaction continues throughout nursing, postweaning and the rest of the pig's life thus shaping the composition of the microbiota. During development, the microbiota can be influenced by several factors including, diet [10], environment [11], weaning [12], antibiotics [13] and probiotics [14].

In order to gain insights into the role played by the microbiota, an understanding of the phylogenetic composition and functional capacity of the microbial community is crucial. With the advent of Next Generation Sequencing techniques, we are able to target and sequence a marker gene such as the 16S ribosomal RNA (16S rRNA) gene in order to describe the phylogenetic composition and diversity of the bacteria and archaea within an environment [15]. And by employing a computational model, such as Phylogenetic Investigation of Communities by Reconstruction of Unobserved States (PICRUSt), we are able to reconstruct microbial metagenomes and ultimately predict metabolic pathways within the communities using only this 16S rRNA gene sequence data and a reference genomes database [16]. While several studies have been done on the microbial communities in the gastrointestinal tract [17,18], the swine oropharyngeal microbiota remains understudied. Interestingly, the oropharynx is in communication with both the digestive and respiratory tracts which are the major routes of infection by pathogenic organisms in the neonatal and weaning stages of life and thus could greatly influence health and performance.

In the current study, we therefore aimed to profile the bacterial composition and predicted metabolic functions of the oropharyngeal microbial community in low and high birthweight piglets and in piglets with low and high average daily gain (ADG) using next generation sequencing. We hypothesized that the rate of weight-gain (ADG) of the heavier piglets would be associated with a characteristic oropharyngeal microbial signature.

MATERIALS AND METHODS

Study animals

The study was conducted on a commercial swine farm with 1,100 breeding sows (Ogeum farm, Yeoju, Korea). A total of 8 mixed sex piglets (3-way crosses; Landrace × Yorkshire × Duroc) born on the same day to two 3rd parity sows were used in the study. Four (4) piglets with a birthweight ≤ 1.0 kg and 4 with a birthweight ≥ 1.7 kg (Table S1), were selected and identified using an oil-based marker that was replenished every week. The body weight of each piglet was measured every week (Table S1), and the average daily gain was calculated by week (Table S2).

The piglets had *ad libitum* access to water and feed throughout the study. At 10 days of age, they were introduced to a creep feed until weaning after which they were graduated to a post weaning diet (see Table S3 and S4 in the supplementary materials). The commercial feed was based on corn and soybean, however, modifications to the texture and relative composition of additives was made as the piglets grew. Minerals, vitamins, enzymes, probiotics and occasionally antibiotics were added to the feed, based on the particular requirements of the co-housed piglets (see Tables S4 and S5). Prophylactic therapies instituted during this period included; Kanamycin administered intranasally at day 1 to control incidences of atrophic rhinitis; vaccinations against *Mycoplasma hyopneumoniae*, Porcine circovirus, *Erysipellothrix rhusiopathiae*, classical swine fever virus as well as against Foot and Mouth disease virus. In addition, colistin was added into the feed.

Sample collection

The oropharyngeal sample was collected by swabbing the soft palate, the root of the tongue and the left and right lateral walls of the oropharyngeal cavity, twice at each surface, using a sterile absorbent swab. The samples were collected at 11, 26, and 63 days of age and stored at −20℃ for about 2 weeks before being transferred to the lab where they were kept at −80℃.

The piglets were individually weighed weekly and records of clinical condition monitored daily. Coughing, sneezing, diarrhoea, general weakness, fur coat texture, injuries among others were monitored.

DNA extraction

DNA from the oropharyngeal swab samples was extracted using the Epicenter MasterPure™ DNA Purification Kit (Epicenter, Madison, WI, USA) following the manufacturer's protocol. First, each sample was rehydrated in 150 μL of autoclaved deionized water in a micro-centrifuge tube at room temperature (25℃) for 30 minutes, vortexed for 15 seconds and then the swab was removed and squeezed against the inside wall of the micro-centrifuge tube. With the resultant solution, the protocol was then followed verbatim. The purity of extracted DNA was assessed by spectrophotometry (NanoDrop Spectrophotometer, Thermo Fisher Scientific, Waltham, MA, USA) through determination of the 260:280 and 260:230 absorbance ratios, while DNA concentration was determined by fluorometry using Qubit HS dsDNA assay kit (Life Technologies, Thermo Fisher Scientific, Waltham, MA, USA). DNA concentration was then normalised to 5 ng/μL and stored at −20℃.

Amplification of bacterial 16S rRNA gene

The V4 hypervariable regions of the bacterial 16S rRNA gene was amplified using the forward primer, 515F (Parada) (5'-GTGYCAGCMGCCGCGGTAA) [19] and the reverse primer, 806R (Apprill) (5'-GGACTACNVGGGTWTCTAAT) [20]. These primers were designed with illumina overhang adapters that are complementary to illumina sequencing primers. The forward overhang nucleotide sequence (5'-TCGTCGGCAGCGTCAGATGTGTATAAGAGACAG-3') was added to the 515F primer while the reverse overhang nucleotide sequence (5'-GTCTCGTGGGCTCGGAGATGTGTATAAGAGACAG-3') was added to the 806R reverse primer. A 25 μL PCR reaction mixture was set up, consisting of 12.5 ng of the DNA template, 1.0 Units of Taq DNA polymerase, 1 μM (5 μL) of each forward and reverse primers, 200 μM of each deoxynucleotide triphosphate (dNTP) and 1x buffer. Along with the PCR reaction, water as a negative control, a known positive control and extraction control reactions were included. The thermocycler was set at an initial denaturation temperature of 95℃ for 3 minutes followed by 25 cycles of 95℃ for 30 seconds, annealing at 56℃ for 30 seconds and elongation at 72℃ for 30 seconds followed by a final elongation for 5 minutes.

The amplicon libraries were cleaned up using Agencourt AMPure XP beads (Beckman Coulter, Brea, CA, USA) according to the manufacturer's protocol and then quantified by fluorometry using Qubit High Sensitivity dsDNA assay kit (Life Technologies, Thermo Fisher Scientific, Waltham, MA, USA).

Genomic DNA library preparation and sequencing

The PCR amplicons were prepared for sequencing by adding indices and illumina sequencing adapters using the Nextera XT DNA index kit (Illumina, San Diego, CA, USA) according to the manufacturer's instructions for single end sequencing. The indexed libraries were then purified using Agencourt AMPure XP beads, quality checked on a Bioanalyzer DNA 1000 chip and then

quantified by fluorometry using Qubit HS dsDNA assay kit. The libraries were then diluted to an equimolar concentration of 4 nM before pooling for sequencing. A final confirmation of the pooled library concentration was done by a fluorometric measurement before denaturing and sequencing. The pooled genomic libraries were then sequenced using the Illumina iSeq 100 platform and using the single-end sequencing method.

Bioinformatics

Analysis was done using QIIME 2 2018.11 [21]. Raw FASTA files were quality filtered and denoised using DADA2 [22] through the q2-dada2 plugin. This involved clipping off of illumina associated adaptor and barcode sequences, followed by trimming of low-quality ends [at 200 base pairs (bp)] as well as removal of low-quality bases. All the sequences were then aligned to the MAFFT [23] and the aligned sequences used to construct a rooted phylogenetic tree using fasttree2 [24] via q2-phylogeny. We then rarefied the samples to 28,076 sequences per sample and estimated alpha diversity metrics, beta diversity metrics and Principle Coordinate Analysis (PCoA) using q2-diversity. The alpha diversity metrics included; Observed operational taxonomic units (OTUs), Evenness, Shannon diversity [25] and Faith's Phylogenetic Diversity [26] while the beta diversity distance matrices included unweighted UniFrac [27], weighted UniFrac [28] and Bray-Curtis dissimilarity [29]. The estimated beta diversity between communities was then visualised using principal coordinate analysis (PCoA) plots. To assign taxonomy to the amplicon sequence variants (ASVs), we used the q2-feature-classifier [30] basing on the classify-sklearn naïve Bayes taxonomy classifier with the Greengenes 13_8 99% OTU's as reference sequences [31]. We assessed the progress of development within the microbiota composition from 11 days through weaning to 63 days of age using q2-longitudinal [32]. Using PICRUSt (phylogenetic Investigation of Communities by Reconstruction of Unobserved States) [16] we predicted KEGG orthology (KO) metagenomes, enzyme commission (EC) metagenomes and MetaCyc pathway abundances through the q2 picrust2 plugin.

Statistical analysis

The data from QIIME 2 was imported into R statistical software [33] for statistical analysis using vegan [34] and Bioconductor packages. To test for statistically significant associations between ADG and relative abundance of genera or pathway abundances, we fit a generalized linear regression using the edgeR package [35]. We corrected for multiple hypothesis testing using the false discovery rafe (FDR) correction method.

Sequence data accession number

All sequence data in this study has been deposited in the NCBI Sequence Read Archive (SRA) database under the BioProject accession number PRJNA602130.

RESULTS

Sequencing data

The twenty-four samples sequenced yielded a total of 3,212,205 sequences ranging from 4 to 284,317 sequences per sample (mean = 133,841.875 and median = 164,482). Quality control and subsequent removal of poor-quality reads in QIIME2 reduced the sequences to a total of 2,390,641 sequences with a mean of 99,610 sequences per sample (ranging from 3 – 243,908 sequences while median = 117,350.5).

Diversity

In order to create an even subsample from each of the samples for calculation of diversity, a sub sampling depth of 28,076 was used. This eliminated 2 samples (B1P2 and B1P5) with fewer reads and left 22 samples with a total of 617,672 reads that were then used to calculate alpha and beta diversities among the samples. The rarefaction plot based on the observed OTU's (Fig. S1) showed a trajectory that initially steeply increased before levelling off at around 40,000 sequences. This indicated that there was good coverage of the communities among all samples.

Taxonomic analysis

The sequences were then clustered into 1,848 OTUs. Taxonomy was assigned by aligning the sequences against the Greengenes 16S rRNA data base at 99% similarity using a Naïve Bayes classifier trained on the V4 hypervariable region. The sequences were dominated by members of the kingdom Bacteria except for two genera belonging to the kingdom Archaea. Proteobacteria and Firmicutes were the most dominant phyla, with a combined relative abundance ranging from 53.17%–97.4% (Fig. 1A). Streptococcaceae, Pasteurellaceae, Moraxellaceae, Veillonellaceae, Neisseriaceae, Leptotrichiaceae, and Lachnospiraceae were the most represented families (Fig. 1B). *Lactobacillaceae* tended to increase in relative abundance post weaning. The most prevalent genera within the samples were *Streptococcus* (Firmicutes) *Actinobacillus* (Proteobacteria), *Moraxella* (Proteobacteria), *Veillonella* (Firmicutes) and *Haemophilus* (Proteobacteria) (Fig. 1C).

## Development of the oropharyngeal microbial community

In order to study the broad changes in microbiota during development, samples were collected at 11, 26, and 63 days of age. Within the first 11 days of life, the piglets' diet was composed entirely of sow milk and creep feeding was initiated at day 12 of life. The samples collected on the 26th day of life represent the oropharyngeal microbial community at the end of nursing. While the samples collected at 63 days of life represented the oropharyngeal microbiota before the end of the weaner stage of life.

PCoA showed that the samples already clustered closely by day 11 of age regardless of maternal or foster sow, that nursed them. Pena Cortes et al. [36] reported a litter effect in the tonsillar microbiota that disappeared by the third week. We did not observe this litter effect by the 11th day of life, probably due to the advancement in age of the piglets in our study compared to those in their study [36]. Further, the samples tended to clusters by age of the piglets except for 2 piglets at 26 days of age, that had been weaned 6 days earlier (Fig. 2). The divergence of the weaned piglets microbiota was expected since weaning stress has been found to disrupt the tonsillar microbial composition [37].

In order to investigate the development pattern influenced by birthweight, we assessed the longitudinal changes in alpha and beta diversity between the birthweight groups (high birthweight, HBW and low birthweight, LBW groups). We found that the Shannon diversity tended to decline between 11 and 26 days of age in both groups of piglets and gradually increased between 26 and 63 days of age (Fig. 3A). Furthermore, we found that the beta diversity tended to change faster in HBW than the LBW piglets during suckling (between 11 and 26 days) (Fig. 3B), however by 63 days of age, the microbiota composition in both groups was relatively equally different from their relative compositions at 11 days of age (Fig. 3C).

Associations between the microbiota and ADG

In order to test whether there was an association between the oropharyngeal microbiota and the ADG of piglets, we run a generalized linear regression using the edgeR package in R. We found 9 genera that were significantly associated with ADG at 11 days of age (FDR < 0.05) and 9 genera
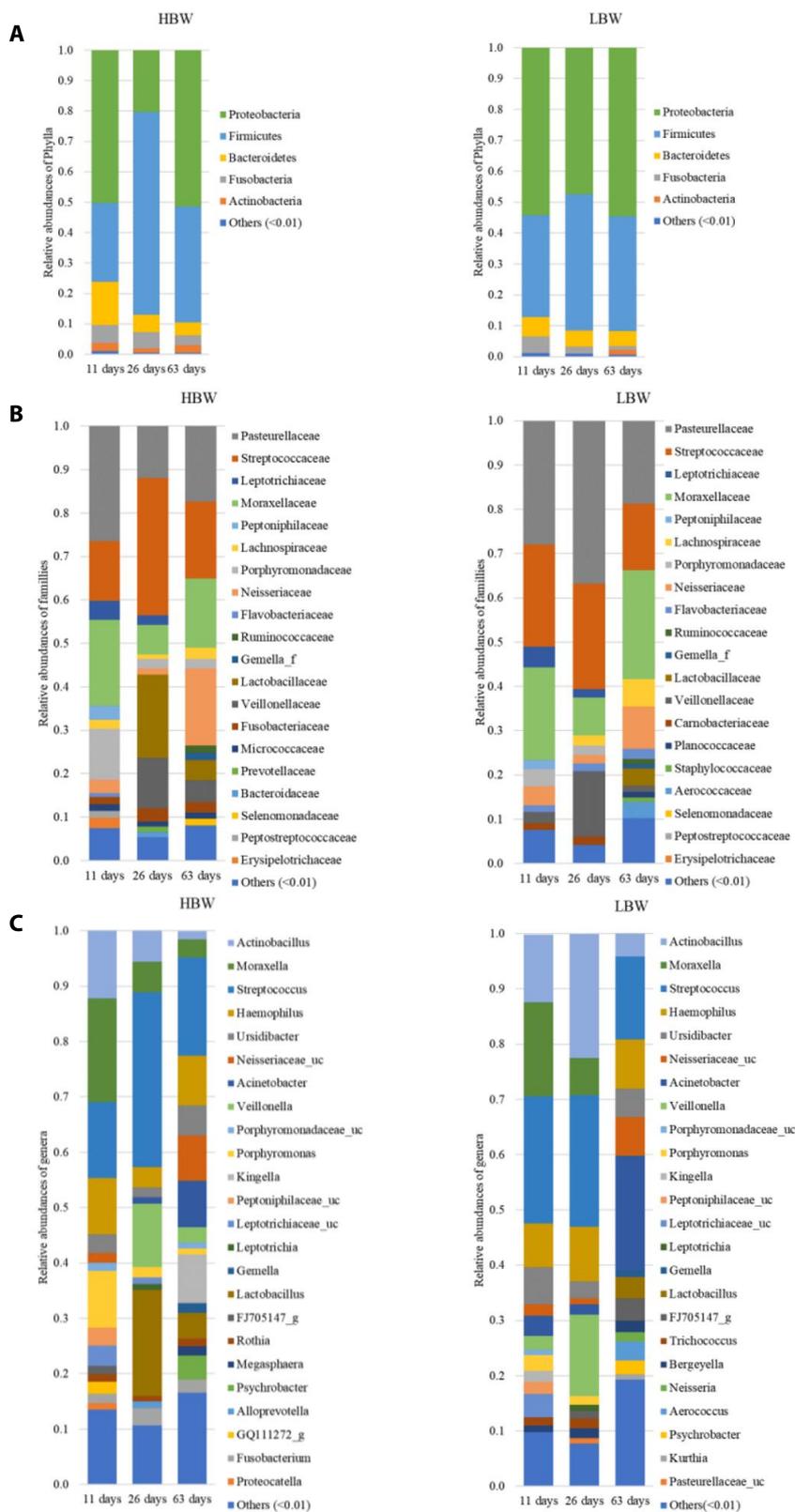
Fig. 1. Stacked bar graphs showing the phylogenetic composition of the oropharyngeal microbiota in high birthweight (HBW) vs low birthweight piglets (LBW) at 11, 26, and 63 days of age. The comparison is made in (A) at phylum level, (B) at family level and (C) at genus level.
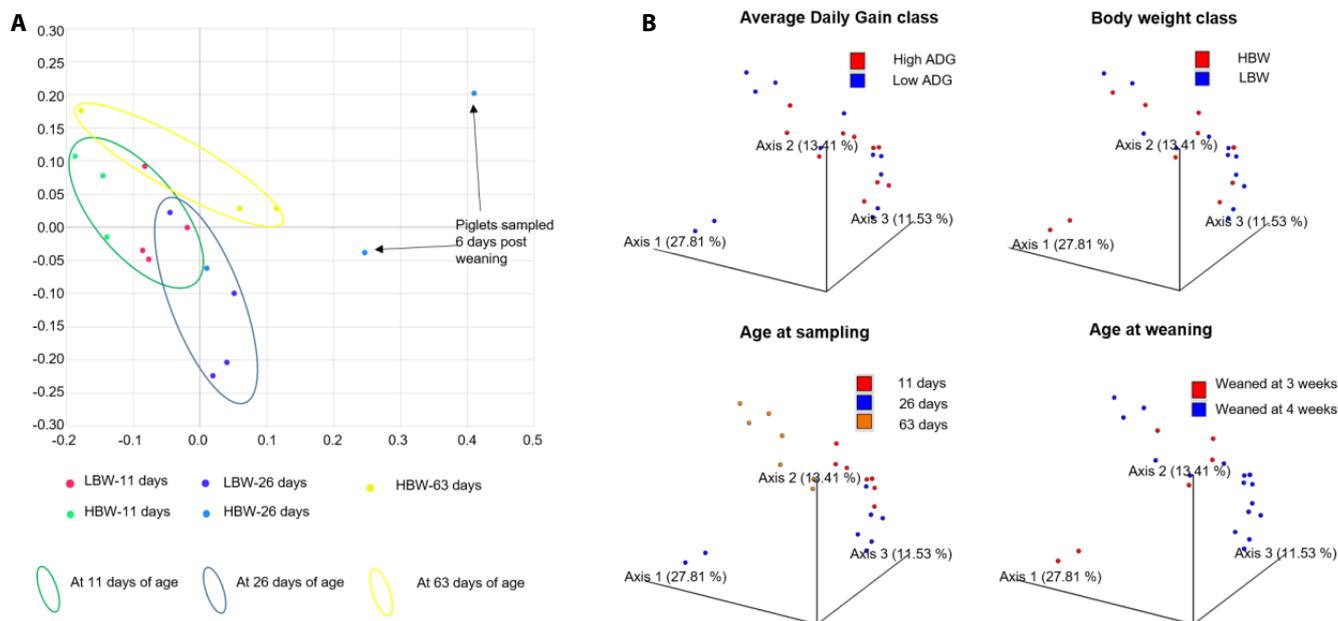
Fig. 2. Principle Coordinate Analysis (PCoA) plots illustrating the phylogenetic composition of the piglets' oropharyngeal microbial community.
(A) Two dimensional PCoA plot based on unweighted UniFrac distances showing the distribution of the microbiota and 95% distribution ellipses at the 3 time points. (B) Three dimensional PCoA plots based on Bray Curtis distances showing the distribution of the oropharyngeal microbiota in samples collected at 11, 26, and 63 days of age. The symbols represent data from individual piglets and are color-coded by the indicated categories of metadata.
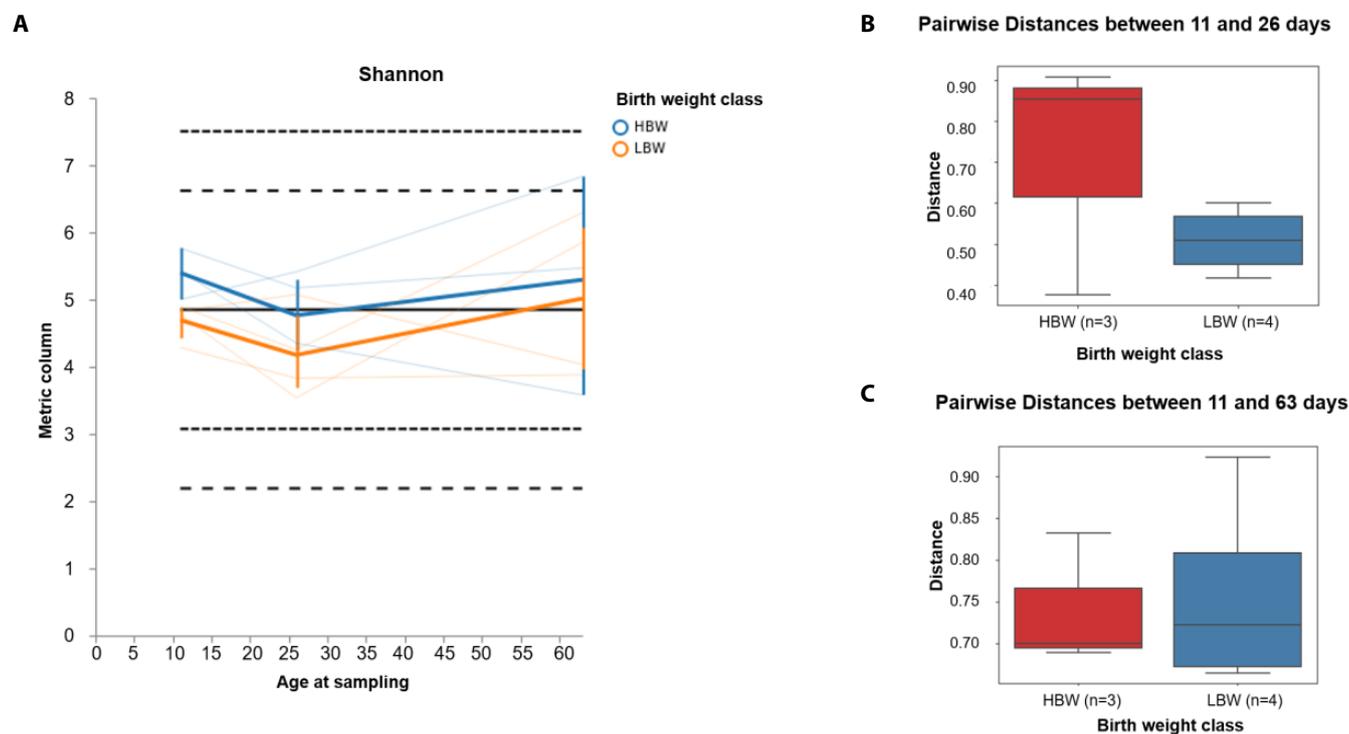
Fig. 3. Longitudinal analysis of microbial composition. In (A) is a volatility plot of Shannon diversity showing changes in alpha diversity in high birth weight (HBW) and in low birth weight (LBW) piglets over the study period. In (B–C) are boxplots showing the paired distances in beta diversity of HBW and LBW piglets; (B) between 11 and 26 days of age and (C) between 11 and 63 days of age. The distances are based on the Bray Curtis distance matrices between each subject's diversity at the given time points.

(FDR < 0.1) at 26 days of age (Table 1 and 2). However, at 63 days of age, no genera were found to be associated with ADG. The association between the microbiota and ADG was stronger earlier in life and reduced post weaning implying that it is potentially more effective to influence weight gain

Table 1. Genera that were significantly associated with ADG at 11 days of age

	Phylum;Class;Order;Family;Genus	logFC	logCPM	LR	*p*-value	FDR
1	Firm;Nega;Vell;Veil;*Veillonella*	−14.67782	16.60199	15.9995	6.34E-05	0.004270
2	Firm;Baci;Lact;Aero;*Aerococcus*	26.99785	14.38829	15.87192	6.78E-05	0.004270
3	Bact;Flav;Flav;[Wee];*Bergeyella*	−37.34028	12.99741	14.98349	0.000108	0.004377
4	Bact;Bact;Bact;[Par];[*Prevotella*]	−18.82124	13.47373	14.85977	0.000116	0.004377
5	Prot;Gamm;Pseu;Mora;*Psychrobacter*	49.12427	13.21755	13.95362	0.000187	0.005902
6	Firm;Baci;Baci;Plan;*Kurthia*	24.61041	8.322315	10.81635	0.001006	0.027109
7	Firm;Baci;Lact;Ente;*Enterococcus*	35.18011	9.889504	10.57308	0.001147	0.027109
8	Prot;Gamm;Pseu;Mora;*Acinetobacter*	18.29274	17.07745	10.1381	0.001452	0.030500
9	Firm;Baci;Lact;Aero;*Facklamia*	19.61991	10.15351	9.796667	0.001748	0.033043
10	Prot;Gamm;Past;Past;*Haemophilus*	−9.712501	14.02468	8.132637	0.004348	0.068474
11	Firm;Baci;Baci;Plan;	39.45043	10.27581	7.677588	0.005591	0.074895
12	Bact;Bact;Bact;[Par];	−27.74231	9.776943	7.637212	0.005718	0.074895
13	Prot;Gamm;Past;Past;*Pasteurella*	−10.47806	11.74235	7.567197	0.005944	0.074895

Nine genera (*Veillonella*, *Aerococcus*, *Bergeyella*, *Prevotella*, *Psychrobacter*, *Kurthia*, *Enterococcus*, *Acinetobacter* and *Facklamia*) within the oropharyngeal microbiota were significantly associated with ADG at 11 days of age (FDR < 0.05).

[ ]; The names in square brackets [ ] within the Greengenes database are still contested at that taxonomic level.

ADG, average daily gain; logFC, log fold-change; logCPM, log counts per million; LR, likelihood ratio; FDR, false discovery rate (adjusted *p*-value).

Phyla; Cyan – Cyanobacteria, Firm – Firmicutes, Bact - Bacteroidetes, Prot – Proteobacteria. **Classes;** Nega – Negativicutes, Baci – Bacilli, Flav – Flavobacteriia, Bact – Bacteroidia, Gamm – Gammaproteobacteria, Alph- Alphaproteobacteria. **Orders;** Vell – Vellionellales, Lact – Lactobacilliales, Flav – Flavobacteriales, Bact – Bacteroidales, Pseu – Pseudomonadales, Baci – Bacillales, Lact – Lactobacillales, Past – Pasteurellales. **Families;** Veil – Veillonellaceae, Aero – Aerococcaceae, Mora – Moraxellaceae, Past – Pasteurellaceae, Plan – Planococcaceae, Past – Pasteurellaceae, Ente – Enterococcaceae.

Table 2. Genera that were significantly associated with ADG at 26 days of age

	Phylum;Class;Order;Family;Genus	logFC	logCPM	LR	*p*-value	FDR
1	Firm;Clos;Clos;[Tis];*Helcococcus*	−23.44355	14.17177	12.71057	0.000364	0.053548
2	Acti;Acti;Acti;Derm;*Helcobacillus*	−25.88382	7.692197	11.72411	0.000617	0.053548
3	Firm;Baci;Lact;Aero;*Aerococcus*	19.01275	14.38829	11.12881	0.00085	0.053548
4	Bact;Bact;Bact;;	−14.66345	15.57125	9.673499	0.001869	0.088331
5	Fuso;Fuso;Fuso;Lept;	−13.97292	14.54914	9.123524	0.002523	0.094253
6	Firm;Erys;Erys;Erys;.1	−16.66539	12.16592	8.465524	0.003619	0.094253
7	Firm;Baci;Lact;Leuc;*Weissella*	16.41927	9.654118	8.248555	0.004078	0.094253
8	Acti;Acti;Acti;Diet;*Dietzia*	33.5106	7.878502	8.101699	0.004422	0.094253
9	Acti;Acti;Acti;Acti;*Arcanobacterium*	−29.88175	10.98488	8.07491	0.004488	0.094253
10	Prot;Gamm;Pseu;Mora;*Psychrobacter*	19.90006	13.21759	7.650028	0.005677	0.107298

Nine genera (*Helcococcus*, *Helcobacillus*, *Aerococcus*, *Weissella*, *Dietzia*, *Arcanobacterium*, and 3 unidentified genera) within the oropharyngeal microbiota were significantly associated with ADG at 26 days of age (FDR < 0.1). Because 3 sequence data of 16S RNA have not been identified in the phylogenetic level of genus in the Greengenes database, they are remarked as 3 unidentified genera.

ADG, average daily gain; logFC, log fold-change; logCPM, log counts per million; LR, likelihood ratio; FDR, false discovery rate (adjusted *p*-value).

[ ]; The name in square bracket [ ] within the Greengenes database is still contested at that taxonomic level.

Phyla; Firm – Firmicutes, Acti - Actinobacteria, Bact - Bacteroidetes, Fuso - Fusobacteria, Prot - Proteobacteria Classes; Clos- Clostridia, Acti - Actinobacteria, Baci - Bacilli, Bact - Bacteroidia, Fuso - Fusobacteriia, Erys - Erysipelotrichia, Gamm – Gammaproteobacteria. **Orders;** Clos- Clostridiales, Acti - Actinomycetales, Lact - Lactobacilliales, Bact – Bacteroidales, Fuso - Fusobacteriales, Erys - Erysipelotrichiales, Pseu – Pseudomonadales. **Families;** Derm - Dermabacteraceae, Aero – Aerococcaceae, Lept - Leptotrichiaceae, Erys - Erysipelotrichaceae, Leuc - Leuconostocaceae, Diet - Dietziaceae, Acti - Actinomycetaceae, Mora – Moraxellaceae.

by manipulating the microbiota earlier in pre-weaning life of the piglets.

Associations between the predicted microbial functional profile and ADG

The association with ADG might be explained better by the metabolic functions performed by the microbial communities in the piglets with diverging ADG's. To investigate this, we used q2picrust2, which uses 16S rRNA gene sequence data to predict the microbial functional repertoire within the samples based on curated reference databases such as the KEGG [38] and MetaCyc [39]. The output from q2picrust2 analysis included predictions of 6,490 KO metagenomes based on the KEGG's Orthologs, 1,980 EC metagenomes and 389 MetaCyc pathway abundances within the 24 samples.

PCoA was used to show the distribution of samples based on the Bray-Curtis distances within their composition of KO metagenomes, EC metagenomes and MetaCyc pathway abundances (Fig. S2). From the PCoA plots it could be seen that weaning had the strongest effect on microbial functional profile and that the samples tended to cluster by age.

We used the MetaCyc pathways output from q2picrust2 to identify metabolic pathways that were associated with ADG in the piglets. To do this we again used a generalized linear regression model within the edgeR package in R. We found 45, 10, and 2 metabolic pathways that were significantly associated with ADG at 11, 26, and 63 days of age, respectively (FDR < 0.05). The MetaCyc pathways found to be significantly associated with ADG were cross referenced with the MetaCyc catalogue [39] to identify their names and the super pathway categories to which they belonged (Tables 3–5).

The pathways associated with ADG belonged to the following categories of super pathways; aromatic compound degradation; nucleoside and nucleotide biosynthesis; nucleoside and nucleotide degradation; sugar nucleotide biosynthesis; sugar acid metabolism, Vitamin K_2 biosynthesis; amino acid biosynthesis; amino acid degradation; amine and polyamine degradation; amine and polyamine biosynthesis; Secondary metabolite degradation; Cell structure biosynthesis; polymyxin resistance; Fatty acid and lipid biosynthesis; Fatty acid Lipid degradation; Inorganic Nutrient Metabolism; Cofactor, prosthetic group, electron carrier and Vitamin biosynthesis; Generation of precursor metabolite and energy; aldehyde degradation; sugar biosynthesis and Antibiotic resistance (Polymyxin resistance) (Tables 3–5).

The aromatic compound degradation category included pathways that are involved in the degradation of Catechol. Apart from the breakdown of xenobiotics, these pathways are capable of degrading the catechol residue derived from the host's catecholamines hormones. Within the nucleoside and nucleotide metabolism pathways, we found that pathways involved in biodegradation significantly increased with ADG during the pre-weaning stage (11 and 26 days of age) while their biosynthesis significantly reduced with increasing ADG (Table 3 and 4). In the Amine and polyamine degradation category, pathways involved in the degradation of allantoin and aromatic biogenic amines increased with ADG while biosynthesis of ectoine decreased with ADG (Table 3). Allantoin is a by-product of purine degradation and therefore it's degradation is connected to the microbes' degradation of nucleotides and nucleosides as a nitrogen source [40,41]. We also observed an increased representation of pathways involved in the degradation of D-glucarate and D-galactarate in high ADG piglets implying that organisms associated with high rates of weight gain have the ability to degrade sugar acids and utilize them as a carbon source for growth (Table 3 and 4).

DISCUSSION

This study investigated the association between the oropharyngeal microbiota and the piglets' birth-

Table 3. Metabolic pathways that were significantly associated with ADG at 11 days of age

	Super pathway	Pathway	logFC	logCPM	LR	*p*-value	FDR
1	Nucleoside and nucleotide biosynthesis	Super pathway of pyrimidine nucleobases salvage	−0.839	13.071	29.653	5.17E-08	2.01E-05
2	Generation of precursor metabolite and Energy	Pentose phosphate pathway (non-oxidative branch)	−0.824	13.094	20.929	4.77E-06	0.000590
3	Aromatic compound degradation	Toluene degradation II (aerobic) (via 4-methylcatechol)	16.045	8.814	20.366	6.40E-06	0.000590
4	Aromatic compound degradation	Toluene degradation I (aerobic) (via o-cresol)	16.044	8.814	20.323	6.54E-06	0.000590
5	Aromatic compound degradation	Catechol degradation I (meta-cleavage pathway)	18.976	8.614	20.040	7.58E-06	0.000590
6	Amine and polyamine degradation	Allantoin degradation to glyoxylate III	14.748	7.650	16.166	5.80E-05	0.003504
7	Inorganic nutrient metabolism	Nitrate reduction VI (assimilatory)	−7.340	9.503	16.009	6.30E-05	0.003504
8	Sugar acid metabolism	D-Galactarate degradation I	8.898	4.542	14.948	0.000111	0.005055
9	Sugar acid metabolism	D-Glucarate and D-galactarate degradation	8.898	4.542	14.841	0.000117	0.005055
10	Aromatic compound degradation	Catechol degradation III (ortho-cleavage pathway)	28.587	8.951	14.399	0.000148	0.005266
11	Aromatic compound degradation	Aromatic compounds degradation via β-ketoadipate	28.588	8.951	14.386	0.000149	0.005266
12	Aromatic compound degradation	Catechol degradation to β-ketoadipate	28.386	8.809	14.070	0.000176	0.005294
13	Fatty acid and lipid biosynthesis	Gondoate biosynthesis (anaerobic)	−0.793	13.048	13.932	0.000190	0.005294
14	Nucleoside and nucleotide degradation	Adenosine nucleotides degradation II	9.844	9.195	13.793	0.000204	0.005294
15	Amino acid degradation	L-Tyrosine degradation I	12.429	8.600	13.747	0.000209	0.005294
16	Amine and polyamine degradation	Aromatic biogenic amine degradation (bacteria)	19.374	6.380	13.671	0.000218	0.005294
17	Aromatic compound degradation	Super pathway of salicylate degradation	26.786	8.625	13.487	0.000240	0.005497
18	Amino acid degradation	L-Leucine degradation I	12.250	9.407	13.213	0.000278	0.005952
19	Nucleoside and nucleotide degradation	Purine nucleotides degradation II (aerobic)	8.390	9.712	13.129	0.000291	0.005952
20	Sugar acid metabolism	D-Glucarate degradation I	8.660	4.806	12.789	0.000349	0.006781
21	Propanoate degradation	2-Methylcitrate cycle I	9.695	8.674	12.467	0.000414	0.007671
22	Aromatic compound degradation	Cinnamate and 3-hydroxycinnamate degradation to 2-hydroxypentadienoate	32.388	8.468	12.098	0.000505	0.008565
23	Aromatic compound degradation	3-Phenylpropanoate and 3-(3-hydroxyphenyl) propanoate degradation to 2-hydroxypentadienoate	32.388	8.468	12.092	0.000506	0.008565
24	Amine and polyamine degradation	Allantoin degradation IV (anaerobic)	13.428	6.716	11.229	0.000805	0.013055
25	Aromatic compound degradation	Meta cleavage pathway of aromatic compounds	22.121	6.813	11.049	0.000888	0.013810
26	Aromatic compound degradation	3-Phenylpropanoate and 3-(3-hydroxyphenyl) propanoate degradation	27.451	8.520	10.975	0.000924	0.013817
27	Secondary metabolite degradation	Engineered pathway: isoprene biosynthesis II (engineered)	12.333	4.357	10.740	0.001048	0.015103
28	Nucleoside and nucleotide biosynthesis	Adenosine ribonucleotides de novo biosynthesis	−0.603	12.960	10.266	0.001355	0.018827
29	Nucleoside and nucleotide biosynthesis	Super pathway of adenosine nucleotides de novo biosynthesis I	−0.693	12.986	10.005	0.001561	0.020945
30	Aromatic compound degradation	4-Methylcatechol degradation (ortho cleavage)	27.042	8.601	9.596	0.001950	0.024940
31	Aromatic compound degradation	Catechol degradation II (meta-cleavage pathway)	12.723	6.818	9.561	0.001988	0.024940
32	Aromatic compound degradation	Protocatechuate degradation II (ortho-cleavage pathway)	10.463	8.309	9.373	0.002202	0.026766
33	Sugar nucleotide biosynthesis	CMP-legionaminate biosynthesis I	−8.205	8.984	9.189	0.002434	0.028639
34	Aromatic compound degradation	Phenylacetate degradation I (aerobic)	20.830	8.727	9.138	0.002503	0.028639
35	Aldehyde degradation	Super pathway of methylglyoxal degradation	21.047	6.569	8.790	0.003029	0.033661
36	Sugar biosynthesis	Sucrose biosynthesis III	18.218	4.108	8.710	0.003165	0.034199
37	Amine and polyamine biosynthesis	Ectoine biosynthesis	15.114	3.587	8.505	0.003543	0.037244
38	Amino acid degradation	L-arginine degradation II (AST pathway)	12.522	4.822	8.097	0.004434	0.045390

Table 3. Continued

	Super pathway	Pathway	logFC	logCPM	LR	*p*-value	FDR
39	Cell structure biosynthesis	Peptidoglycan biosynthesis II (staphylococci)	4.900	9.105	7.908	0.004922	0.048418
40	Nucleoside and nucleotide biosynthesis	Super pathway of adenosine nucleotides de novo	–0.697	12.922	7.853	0.005073	0.048418
41	Cell structure biosynthesis	UDP-N-acetylmuramoyl-pentapeptide biosynthesis I (meso-diaminopimelate containing)	–0.739	12.817	7.781	0.005280	0.048418
42	Secondary metabolite degradation	Sulfoquinovose degradation I	10.149	3.185	7.742	0.005395	0.048418
43	Aromatic compound degradation	Catechol degradation to 2-hydroxypentadienoate II	11.213	6.438	7.732	0.005425	0.048418
44	Amino acid biosynthesis	L-Lysine biosynthesis II	–2.476	11.855	7.715	0.005477	0.048418
45	Antibiotic resistance	Polymyxin resistance	9.731	3.860	7.668	0.005621	0.048588

ADG, average daily gain; logFC, log fold-change; logCPM, log counts per million; LR, likelihood ratio; FDR, false discovery rate (adjusted *p*-value).

Table 4. Metabolic pathways that were significantly associated with ADG at 26 days of age

	Super pathway	Pathway	logFC	logCPM	LR	*p*-value	FDR
1	Aromatic compound degradation	Catechol degradation I (meta-cleavage pathway)	15.28376	8.613798	19.28901	1.12E-05	0.00437
2	Aromatic compound degradation	Catechol degradation to 2-hydroxypentadienoate II	12.99083	6.437917	15.3016	9.16E-05	0.0148
3	Aromatic compound degradation	Catechol degradation II (meta-cleavage pathway)	12.94294	6.817753	14.8872	0.000114	0.0148
4	Fatty acid and lipid biosynthesis	Super pathway of lipopolysaccharide biosynthesis	28.38013	2.42697	13.50893	0.000237	0.02309
5	Aromatic compound degradation	Toluene degradation II (aerobic) (via 4-methylcatechol)	10.58863	8.813538	12.74445	0.000357	0.023322
6	Aromatic compound degradation	Toluene degradation I (aerobic) (via o-cresol)	10.58859	8.813538	12.73057	0.00036	0.023322
7	Sugar acid metabolism	D-Galactarate degradation I	8.848847	4.542388	11.51003	0.000692	0.031156
8	Antibiotic resistance	Polymyxin resistance	15.29624	3.859829	11.46961	0.000707	0.031156
9	Sugar acid metabolism	Super pathway of D-glucarate and D-Galactarate degradation	8.848833	4.542388	11.43476	0.000721	0.031156
10	Nucleoside and nucleotide biosynthesis	Super pathway of pyrimidine nucleobases salvage	–0.46889	13.07049	10.52772	0.001176	0.045745
11	Sugar acid metabolism	D-glucarate degradation I	8.936948	4.805885	10.33191	0.001307	0.046238
12	Amine and polyamine degradation	Allantoin degradation IV (anaerobic)	12.94646	6.715548	9.796436	0.001749	0.051378

ADG, average daily gain; logFC, log fold-change; logCPM, log counts per million; LR, likelihood ratio; FDR, false discovery rate (adjusted *p*-value).

Table 5. Metabolic pathways that were significantly associated with ADG at 63 days of age

	Super pathway	Pathway	logFC	logCPM	LR	*p*-value	FDR
1	Vitamin K_2 biosynthesis	1,4-Dihydroxy-6-naphthoate biosynthesis I	43.60243	5.323691	13.81177	0.000202	0.041719
2	Inorganic nutrient metabolism	Super pathway of sulphur oxidation (*Acidianus ambivalens*)	27.23389	8.525369	13.69964	0.000214	0.041719
3	Fatty acid and lipid degradation	Phospholipase pathway	–48.3973	–0.97698	12.20301	0.000477	0.061867
4	Vitamin K_2 biosynthesis	1,4-Dihydroxy-6-naphthoate biosynthesis II	28.17554	6.774948	10.42818	0.001241	0.120694
5	Aromatic compound degradation	Catechol degradation to 2-hydroxypentadienoate II	17.00923	6.437778	7.659094	0.005649	0.407778

ADG, average daily gain; logFC, log fold-change; logCPM, log counts per million; LR, Likelihood ratio; FDR, False discovery rate (adjusted *p*-value).

weight and rate of weight gain. Results revealed microbial clades and pathways that were associated with the piglets' weight gain. However, the associations were stronger in the pre-weaning phase and appeared to wane with age implying that an attempt to improve weight gain through modulation of the microbiota should target early life of the piglet, particularly before 4 weeks of life.

Our findings from the taxonomic analysis of the oropharyngeal microbiota were largely in

agreement with studies focusing on the tonsillar microbiota [36,42,43]. However, the dominance of *Streptococcus*, in our study, was striking since it was only represented as a minor community member within the tonsils [42]. It has been found that the catecholamine stress hormones, norepinephrine (NOR) and dopamine (DOP), induce the proliferation of some species of *Streptococcus* [44]. In our study, the piglets were raised under a commercial farm setting, which is characterized by cross fostering, weaning and frequent regrouping of the piglets. These events involve changing the piglets environment and disruption of their social structure, consequently elevating the levels of circulating catecholamines [45]. In addition, Pasteurella, which was found to dominate in the tonsillar microbial communities [42] had a surprisingly low relative abundance among our samples (1% or less). These slight differences can partly be explained by the fact that the above studies focused on the tonsillar microbiota while this study included pooled samples of the oropharyngeal cavity.

We did not find any statistically significant difference between the development of oropharyngeal microbiota in HBW and LBW piglets. However, we found subtle differences that tended to disappear by 63 days of life implying that birthweight only had a slight effect on the oropharyngeal microbiota during the first few weeks of pre-weaning which gradually wanes as the piglets grow older. In contrast to our findings, studies done in the piglets' gut have found statistically significant differences between the microbiota of low birthweight and normal birthweight piglets during the pre-weaning phase [46,47]. However, these differences also tended to disappear by 35 days of age [46].

The current trend in microbiome research has been to explore the microbial metabolic functions that may have clinical, therapeutic or nutritional relevance to the host [48]. Previous studies in domestic pigs have reported correlations between feed efficiency and the illeal, caecal, colonic and fecal microbiome [49–51]. In this study, we explored the association between the predicted metabolic pathways within the oropharyngeal microbiome and ADG in the piglets. Our results showed an enrichment of pathways involved in the biodegradation of nucleosides and nucleotides in heavier piglets during the pre-weaning phase. The reason for this association is not clear, however one possible explanation could be, that the relationship is a consequence, and not a cause, of the ADG among the piglets. It is known that sow milk, like all mammalian milk is a very rich source of nucleosides [52]. It is therefore possible that, as a result of their competitive advantage, the larger piglets have more access to the best teats and also spend more time suckling [53] resulting in a consistently higher concentration of sow milk-derived nucleosides within the saliva matrix in their oropharynx. This would then favor the proliferation of bacteria with the ability to utilize nucleosides and nucleotides. On the other hand, members of the oropharyngeal microbiota within the lighter piglets have to biosynthesize their nucleotides and nucleosides to sustain their growth and proliferation.

The association of catechol degradation pathways with ADG, suggests an enhanced ability to degrade host derived catecholamines within the oropharyngeal microbiome of piglets having high rates of weight gain. Catecholamines, which include Dopamine (DOP), Epinephrine (EPI) and Norepinephrine (NOR), are secreted during stressful conditions [54]. It is likely that the high ADG piglets have higher appetite levels compared to the low ADG piglets and are therefore more inclined towards aggression and competition for feed with their pen mates leading to higher levels of stress hormones (EPI and NOR) within their circulation [55,56]. Circulating catecholamines are partly secreted into the saliva matrix and this may lead to an accumulation of bacteria, within the oropharynx, that have the ability to degrade catechols. Catecholamines are also involved in the regulation of hedonic feeding in mammals [57]. Hedonic feeding refers to the non-homeostatic feeding that is not driven by energy requirements but simply driven by pleasure or desire to consume palatable feed [58]. Some catecholamines have been shown to induce feeding behavior such as food-anticipatory activity, search for food and motivation to feed [59]. Breakdown of these

catecholamines, interferes with systemic regulation of their production [60]. Interfering with the feedback control of the central catecholamine release could then lead to a sustained secretion and consequently, a sustained appetitive feeding in pigs thus contributing to attainment of higher rates of weight gain.

In summary, we identified microbial biomarkers within the oropharyngeal microbiome that may be used as targets for modulating rates of weight gain in piglets. However, our study does not confirm whether the detected microbial signature is a cause or an effect of the ADG therefore, requiring further studies. In future, studies that employ 'omics' techniques are needed in order to better understand the roles played by this oropharyngeal microbiota. Combining techniques that can reveal the active genes (transcriptomics), synthesized protein molecules (proteomics) and their metabolic products (metabolomics) could provide deeper insights into the role of this oropharyngeal microbiome.

SUPPLEMENTARY MATERIALS

Supplementary materials are only available online from: https://doi.org/10.5187/jast.2020.62.2.247

REFERENCES

1. Quiniou N, Dagorn J, Gaudré D. Variation of piglets' birth weight and consequences on subsequent performance. Livest Prod Sci. 2002;78:63-70.
2. Douglas SL, Wellock I, Edwards SA, Kyriazakis I. High specification starter diets improve the performance of low birth weight pigs to 10 weeks of age. J Anim Sci. 2014;92:4741-50.
3. Li J. Current status and prospects for in-feed antibiotics in the different stages of pork production: a review. Asian-Australas J Anim Sci. 2017;30:1667-73.
4. Schokker D, Zhang J, Zhang LL, Vastenhouw SA, Heilig HG, Smidt H, et al. Early-life environmental variation affects intestinal microbiota and immune development in new-born piglets. PLoS One. 2014;9:e100040.
5. Sommer F, Bäckhed F. The gut microbiota-masters of host development and physiology. Nat Rev Microbiol. 2013;11:227-38.
6. Turnbaugh PJ, Ley RE, Mahowald MA, Magrini V, Mardis ER, Gordon JI. An obesity-associated gut microbiome with increased capacity for energy harvest. Nature. 2006;444:1027-31.
7. Mikov M. The metabolism of drugs by the gut flora. Eur J Drug Metab Pharmacokinet. 1994;19:201-7.
8. Kim JS, de La Serre CB. Diet, gut microbiota composition and feeding behavior. Physiol Behav. 2018;192:177-81.
9. Mackie RI, Sghir A, Gaskins HR. Developmental microbial ecology of the neonatal gastrointestinal tract. Am J Clin Nutr. 1999;69:1035S-45S.
10. Heinritz SN, Weiss E, Eklund M, Aumiller T, Heyer CM, Messner S, et al. Impact of a high-fat or high-fiber diet on intestinal microbiota and metabolic markers in a pig model. Nutrients. 2016;8:317.
11. Thompson CL, Wang B, Holmes AJ. The immediate environment during postnatal development has long-term impact on gut community structure in pigs. ISME J. 2008;2:739-48.
12. Guevarra RB, Hong SH, Cho JH, Kim BR, Shin J, Lee JH, et al. The dynamics of the piglet gut microbiome during the weaning transition in association with health and nutrition. J Anim Sci Biotechnol. 2018;9:54.
13. Yu M, Mu C, Zhang C, Yang Y, Su Y, Zhu W. Marked response in microbial community and

metabolism in the ileum and cecum of suckling piglets after early antibiotics exposure. Front Microbiol. 2018;9:1166.

14. Shim SB, Verstegen MW, Kim IH, Kwon OS, Verdonk JM. Effects of feeding antibiotic-free creep feed supplemented with oligofructose, probiotics or synbiotics to suckling piglets increases the preweaning weight gain and composition of intestinal microbiota. Arch Anim Nutr. 2005;59:419-27.

15. Liu L, Li Y, Li S, Hu N, He Y, Pong R, et al. Comparison of next-generation sequencing systems. J Biomed Biotechnol. 2012. doi:10.1155/2012/251364.

16. Langille MGI, Zaneveld J, Caporaso JG, McDonald D, Knights D, Reyes JA, et al. Predictive functional profiling of microbial communities using 16S rRNA marker gene sequences. Nat Biotechnol. 2013;31:814-21.

17. Mach N, Berri M, Estellé J, Levenez F, Lemonnier G, Denis C, et al. Early-life establishment of the swine gut microbiome and impact on host phenotypes. Environ Microbiol Rep. 2015;7:554-69.

18. Konstantinov SR, Awati AA, Williams BA, Miller BG, Jones P, Stokes CR, et al. Post-natal development of the porcine microbiota composition and activities. Environ Microbiol. 2006;8:1191-9.

19. Parada AE, Needham DM, Fuhrman JA. Every base matters: assessing small subunit rRNA primers for marine microbiomes with mock communities, time series and global field samples. Environ Microbiol. 2016;18:1403-14.

20. Apprill A, McNally S, Parsons R, Weber L. Minor revision to V4 region SSU rRNA 806R gene primer greatly increases detection of SAR11 bacterioplankton. Aquat Microb Ecol. 2015;75:129-37.

21. Bolyen E, Rideout JR, Dillon MR, Bokulich NA, Abnet C, Al-Ghalith GA, et al. Reproducible, interactive, scalable and extensible microbiome data science using QIIME 2. Nat Biotechnol. 2019;37:852–7.

22. Callahan BJ, McMurdie PJ, Rosen MJ, Han AW, Johnson AJA, Holmes SP. DADA2: high-resolution sample inference from Illumina amplicon data. Nat Methods. 2016;13:581-3.

23. Katoh K, Misawa K, Kuma K, Miyata T. MAFFT: a novel method for rapid multiple sequence alignment based on fast Fourier transform. Nucleic Acids Res. 2002;30:3059-66.

24. Price MN, Dehal PS, Arkin AP. FastTree 2: approximately maximum-likelihood trees for large alignments. PLoS One. 2010;5:e9490.

25. Shannon CE. A mathematical theory of communication. Bell Syst Tech J. 1948;27:379-423.

26. Faith DP. Conservation evaluation and phylogenetic diversity. Biol Conserv. 1992;61:1-10.

27. Lozupone C, Knight R. UniFrac: a new phylogenetic method for comparing microbial communities. Appl Environ Microbiol. 2005;71:8228-35.

28. Lozupone CA, Hamady M, Kelley ST, Knight R. Quantitative and qualitative beta diversity measures lead to different insights into factors that structure microbial communities. Appl Environ Microbiol. 2007;73:1576-85.

29. Bray JR, Curtis JT. An ordination of the upland forest communities of Southern Wisconsin. Ecol Monogr. 1957;27:325-49.

30. Bokulich NA, Kaehler BD, Rideout JR, Dillon M, Bolyen E, Knight R, et al. Optimizing taxonomic classification of marker-gene amplicon sequences with QIIME 2's q2-feature-classifier plugin. Microbiome. 2018;6:90.

31. McDonald D, Price MN, Goodrich J, Nawrocki EP, DeSantis TZ, Probst A, et al. An improved Greengenes taxonomy with explicit ranks for ecological and evolutionary analyses of bacteria and archaea. ISME J. 2012;6:610-8.

32. Bokulich NA, Dillon MR, Zhang Y, Rideout JR, Bolyen E, Li H, et al. q2-longitudinal: longitudinal and paired-sample analyses of microbiome data. mSystems. 2018;3:e00219-18.

33. R Core Team. R: a language and environment for statistical computing. Vienna, Austria: R Foundation for Statistical Computing.

34. Dixon P. VEGAN, a package of R functions for community ecology. J Veg Sci. 2003;14:927-30.

35. Robinson MD, McCarthy DJ, Smyth GK. edgeR: a bioconductor package for differential expression analysis of digital gene expression data. Bioinformatics. 2010;26:139-40.

36. Cortes LCP, LeVeque RM, Funk J, Marsh TL, Mulks MH. Development of the tonsillar microbiome in pigs from newborn through weaning. BMC Microbiol. 2018;18:35.

37. Cortes LCP, LeVeque RM, Funk JA, Marsh TL, Mulks MH. Development of the tonsil microbiome in pigs and effects of stress on the microbiome. Front Vet Sci. 2018;5:220.

38. Kanehisa M, Sato Y, Furumichi M, Morishima K, Tanabe M. New approach for understanding genome variations in KEGG. Nucleic Acids Res. 2019;47:D590-5.

39. Caspi R, Altman T, Billington R, Dreher K, Foerster H, Fulcher CA, et al. The MetaCyc database of metabolic pathways and enzymes and the BioCyc collection of pathway/genome databases. Nucleic Acids Res. 2014;42:D459-71.

40. Cusa E, Obradors N, Baldomà L, Badía J, Aguilar J. Genetic analysis of a chromosomal region containing genes required for assimilation of allantoin nitrogen and linked glyoxylate metabolism in Escherichia coli. J Bacteriol. 1999;181:7479-84.

41. Vogels GD, Van der Drift C. Degradation of purines and pyrimidines by microorganisms. Bacteriol Rev. 1976;40:403-68.

42. Lowe BA, Marsh TL, Isaacs-Cosgrove N, Kirkwood RN, Kiupel M, Mulks MH. Defining the "core microbiome" of the microbial communities in the tonsils of healthy pigs. BMC Microbiol. 2012;12:20.

43. Mann E, Pinior B, Wetzels SU, Metzler-Zebeli BU, Wagner M, Schmitz-Esser S. The metabolically active bacterial microbiome of tonsils and mandibular lymph nodes of slaughter pigs. Front Microbiol. 2015;6:1362.

44. Sandrini S, Alghofaili F, Freestone P, Yesilkaya H. Host stress hormone norepinephrine stimulates pneumococcal growth, biofilm formation and virulence gene expression. BMC Microbiol. 2014;14:180.

45. Colson V, Martin E, Orgeur P, Prunier A. Influence of housing and social changes on growth, behaviour and cortisol in piglets at weaning. Physiol Behav. 2012;107:59-64.

46. Li N, Huang S, Jiang L, Wang W, Li T, Zuo B, et al. Differences in the gut microbiota establishment and metabolome characteristics between low- and normal-birth-weight piglets during early-life. Front Microbiol. 2018;9:1798.

47. Li N, Huang S, Jiang L, Dai Z, Li T, Han D, et al. Characterization of the early life microbiota development and predominant lactobacillus species at distinct gut segments of low- and normal-birth-weight piglets. Front Microbiol. 2019;10:797.

48. Arnold JW, Roach J, Azcarate-Peril MA. Emerging technologies for gut microbiome research. Trends Microbiol. 2016;24:887-901.

49. Quan J, Cai G, Ye J, Yang M, Ding R, Wang X, et al. A global comparison of the microbiome compositions of three gut locations in commercial pigs with extreme feed conversion ratios. Sci Rep. 2018;8:4536.

50. Tan Z, Yang T, Wang Y, Xing K, Zhang F, Zhao X, et al. Metagenomic analysis of cecal microbiome identified microbiota and functional capacities associated with feed efficiency in landrace finishing pigs. Front Microbiol. 2017;8:1546.

51. Yang H, Huang X, Fang S, He M, Zhao Y, Wu Z, et al. Unraveling the fecal microbiota and metagenomic functional capacity associated with feed efficiency in pigs. Front Microbiol. 2017;8:1555.

52. Mateo CD, Peters DN, Stein HH. Nucleotides in sow colostrum and milk at different stages of lactation. J Anim Sci. 2004;82:1339-42.

53. Drake A, Fraser D, Weary DM. Parent-offspring resource allocation in domestic pigs. Behav Ecol Sociobiol. 2008;62:309-19.

54. Munck A, Guyre PM, Holbrook NJ. Physiological functions of glucocorticoids in stress and their relation to pharmacological actions. Endocr Rev. 1984;5:25-44.

55. Arnone M, Dantzer R. Does frustration induce aggression in pigs? Appl Anim Ethol. 1980;6:351-62.

56. Martínez-Miró S, Tecles F, Ramón M, Escribano D, Hernández F, Madrid J, et al. Causes, consequences and biomarkers of stress in swine: an update. BMC Vet Res. 2016;12:171.

57. Blundell J. Pharmacological approaches to appetite suppression. Trends Pharmacol Sci. 1991;12:147-57.

58. Rossi MA, Stuber GD. Overlapping brain circuits for homeostatic and hedonic feeding. Cell Metab. 2018;27:42-56.

59. Smit AN, Patton DF, Michalik M, Opiol H, Mistlberger RE. Dopaminergic regulation of circadian food anticipatory activity rhythms in the rat. PLoS One. 2013;8:e82381.

60. Eisenhofer G, Kopin IJ, Goldstein DS. Catecholamine metabolism: a contemporary view with implications for physiology and medicine. Pharmacol Rev. 2004;56:331-49.

SUPPLEMENTARY MATERIALS

Table S1. Body weights of piglets during the study

ID	Sex	Uc	B-O	MS	FS	Wean-age	BW-class	Body-weight (kg) / day of age										
								0 d	7 d	11 d	14 d	21 d	27 d	35 d	42 d	49 d	55 d	63 d
R1	M	33	5	A	D	20	HBW	2.1	4.4	5.0	5.6	6.6	7.6	11.4	14.1	16.4	20.5	24.5
R2	F	27	6	A	D	20	HBW	1.8	2.9	3.5	4.3	5.1	5.9	9.1	12.6	15.4	18.4	22.5
R3	F		9	A	E	27	LBW	1.0	2.0	2.8	3.5	5.1	6.3	6.8	9.4	11.9	14.7	17.0
R4	F	25	12	A	E	27	LBW	0.9	2.4	3.3	4.2	5.9	7.3	8.4	10.6	13.2	16.0	19.0
B1	M	26	1	B	F	26	HBW	1.7	3.4	4.7	5.8	7.9	9.8	11.0	13.7	15.2	17.2	20.5
B2	M	40	5	B	F	26	HBW	1.7	3.2	4.4	5.5	7.0	8.4	8.9	11.4	12.7	14.6	17.6
B3	F	37	6	B	B	26	LBW	1.0	2.0	2.7	3.4	4.5	5.6	8.1	11.2	13.3	16.7	20.5
B6	F	27	12	B	B	26	LBW	1.0	2.2	3.2	4.0	5.0	6.2	8.5	11.6	14.7	17.8	22.7

ID, piglet's identification; Uc, umbilical cord circumference (mm); B-O, birth order; MS, maternal sow (A and B); FS, foster sow (D, E, and F); Wean-age, age at weaning (days); BW-Class, birthweight class category; HBW, high birthweight; LBW, low birthweight.

In this study, we classified a pig as heavy (H) or light (L) at the point of sampling basing on the following criteria;

	Weight range	Bodyweight class
At day 11	≤ 3.4	L
	≥ 3.5	H
At day 27	≤ 6.9	L
	≥ 7.0	H
At day 63	≤ 19.9	L
	≥ 20.0	H

Table S2. Average daily gains of piglets during the study

ID	Sex	Uc	B-O	MS	FS	Wean-age	Average daily gain (ADG) / day of age									
							7 d	11 d	14 d	21 d	27 d	35 d	42d	49 d	55 d	63 d
R1	M	33	5	A	D	20	0.331	0.250	0.174	0.143	0.167	0.475	0.386	0.329	0.683	0.500
R2	F	27	6	A	D	20	0.146	0.180	0.206	0.114	0.133	0.400	0.500	0.400	0.500	0.513
R3	F	-	9	A	E	27	0.141	0.170	0.217	0.229	0.200	0.063	0.371	0.357	0.467	0.288
R4	F	25	12	A	E	27	0.214	0.240	0.257	0.243	0.233	0.138	0.314	0.371	0.467	0.375
B1	M	26	1	B	F	26	0.287	0.320	0.346	0.300	0.317	0.150	0.386	0.214	0.333	0.413
B2	M	40	5	B	F	26	0.248	0.290	0.330	0.214	0.233	0.063	0.357	0.186	0.317	0.375
B3	F	37	6	B	B	26	0.158	0.180	0.207	0.157	0.183	0.313	0.443	0.300	0.567	0.475
B6	F	27	12	B	B	26	0.207	0.230	0.251	0.143	0.200	0.288	0.443	0.443	0.517	0.613

ID, piglet's identification; Uc, umbilical cord circumference (mm); B-O, birth order; MS, maternal sow (A and B); FS, foster sow (D, E, and F); Wean-age, age at weaning (days).

In this study, ADG values were categorised as either low ADG (ldg) or high ADG (hdg) as indicated below.

	ADG range	ADG class
At day 11	≤ 0.19	ldg
	≥ 0.20	hdg
At day 27	≤ 0.22	ldg
	≥ 0.23	hdg
At day 63	≤ 0.49	ldg
	≥ 0.50	hdg

Table S3. Dietary composition of creep, starter and milk replacer

Creep feed ingredients	Amount
D100	1 kg
Probiotic 1	10 g
Probiotic 2	2.5 g
Vitamin mix 1	5 g
Colistin[1]	2.5 g
Minerals	5 g
Starter feed ingredients	
D100	1 kg
Probiotic 2	1.25 g
Minerals	1.25 g
Probiotic 1	3.75 g
Vitamin mix 1	1.25 g
Colistin[1]	1.25 g
D100 Milk replacer (MR) approximate composition	
Crude protein	16.50%
Crude fat	13.00%
Crude fibre	1.00%
Crude ash	4.00%
Ca	0.30%
P	0.50%
Lysine	1.50%
Digestible energy	4,750 kcal/kg
Digestible crude protein	14.00%

[1]The Colistin formulation contained colistin sulphate at a concentration of 20 g/kg.

Table S4. Weaner feeding schedule

Approx. age (d)	Days post-weaning	Ingredients
28–29	1–2	Starter feed
30–32	3–5	D100 + D200 (1:1)
		Probiotic 1 (5 g/kg of feed)
33–39	6–12	D 200
		Colistin[1] (2.5 g/kg of feed)
		Probiotic 1 (5 g/kg of feed)
40–42	13–15	D200 + D300 (1:1)
		Probiotic 1 (2 g/kg of feed)
		Organic acids (2 g/kg of feed)
43–48	16–21	D300
		Ivermectin[2] (0.333 g/kg of feed)
		Probiotic 1 (2 g/kg of feed)
48–51	21–24	D300 + 3H (1:1)
		Enrofloxacin (1 g/kg of feed)
		Ivermectin[2] (0.333 g/kg of feed)
		Probiotic 1 (2 g/kg of feed)
52–70	25	3H
		Probiotic 1 (2 g/kg of feed)

Throughout the study the animals had *ad libitum* access to the feed rations.

[1]The Colistin formulation contained colistin sulphate at a concentration of 20 g/kg.

[2]The Ivermectin formulation contained active Ivermectin at a concentration of 6.12 g/kg.

Table S5. Additives and their compositions

| Vitamin mix 1		Probiotic 1	
Ingredients	(per kg)	*Bacillus* spp.	1.0×10^9 cfu/kg
Vitamin A	6,000,000 IU	*Lactobacillus* spp.	1.0×10^9 cfu/kg
Vitamin D_3	600,000 IU	*Saccharomyces* spp.	1.0×10^9 cfu/kg
Vitamin E	1,000 IU	**Probiotic 2**	
Vitamin K_3	500 mg	*Clostridium butyricum*	1.0×10^{10} cfu/kg
Vitamin B_1	97 mg	Lactose hydrate	
Vitamin B_2	600 mg	Glucose	
Vitamin B_6	400 mg	**Organic acids**	**Per kg**
Vitamin B_{12}	400 ug	Formic acid	300,000 mg
Nicotinic acid	2,400 mg	Citric acid	100,000 mg
Biotin	40 mg	Propionic acid	50,000 mg
Choline chloride	25,000 mg	Malic acid	50,000 mg
Folic acid	200 mg	Complex amino acids	> 25%
$MgSO_4$	4,000 mg	**Minerals**	
Ca-pantothenate	1,000 mg	Zn	2.70%
$FeSO_4$	8,000 mg	Cu	1.70%
$ZnSO_4$	230,000 mg	Mn	1.30%
$CuSO_4$	1,000 mg	Fe	1.30%
$MnSO_4$	12,000 mg	Cr	160 ppm
$CaCO_3$	800 mg		
Ca-iodine	500 mg		
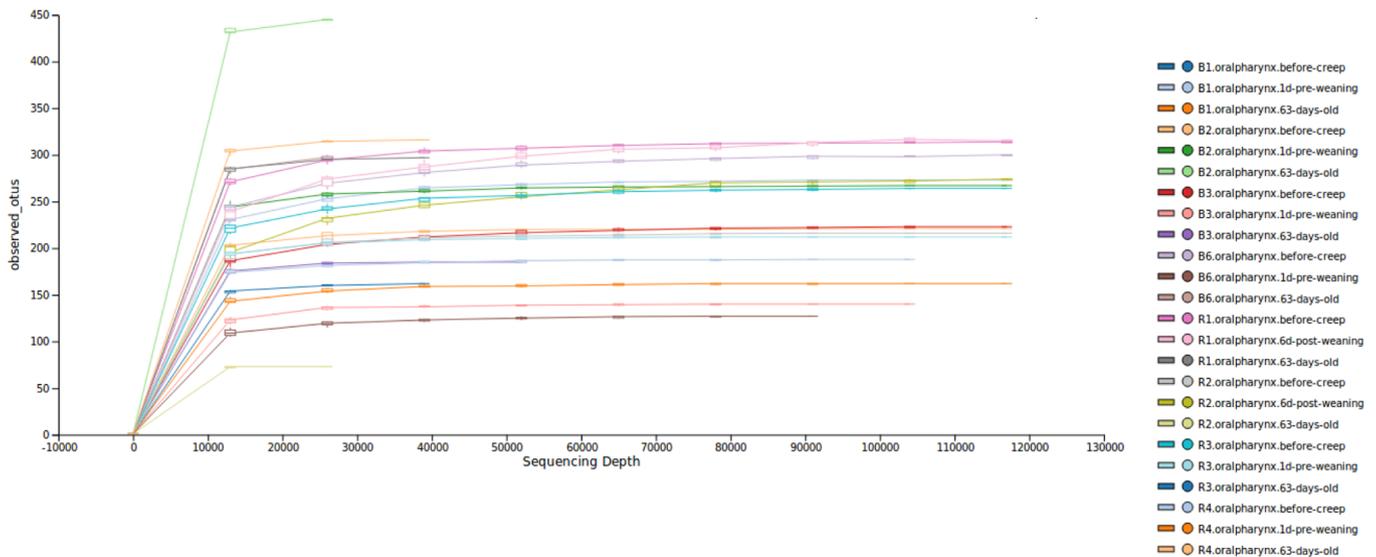
Fig. S1. **Alpha rarefaction plot based on observed OTU's showing efficiency of sampling.** OTU, operational taxonomic unit.
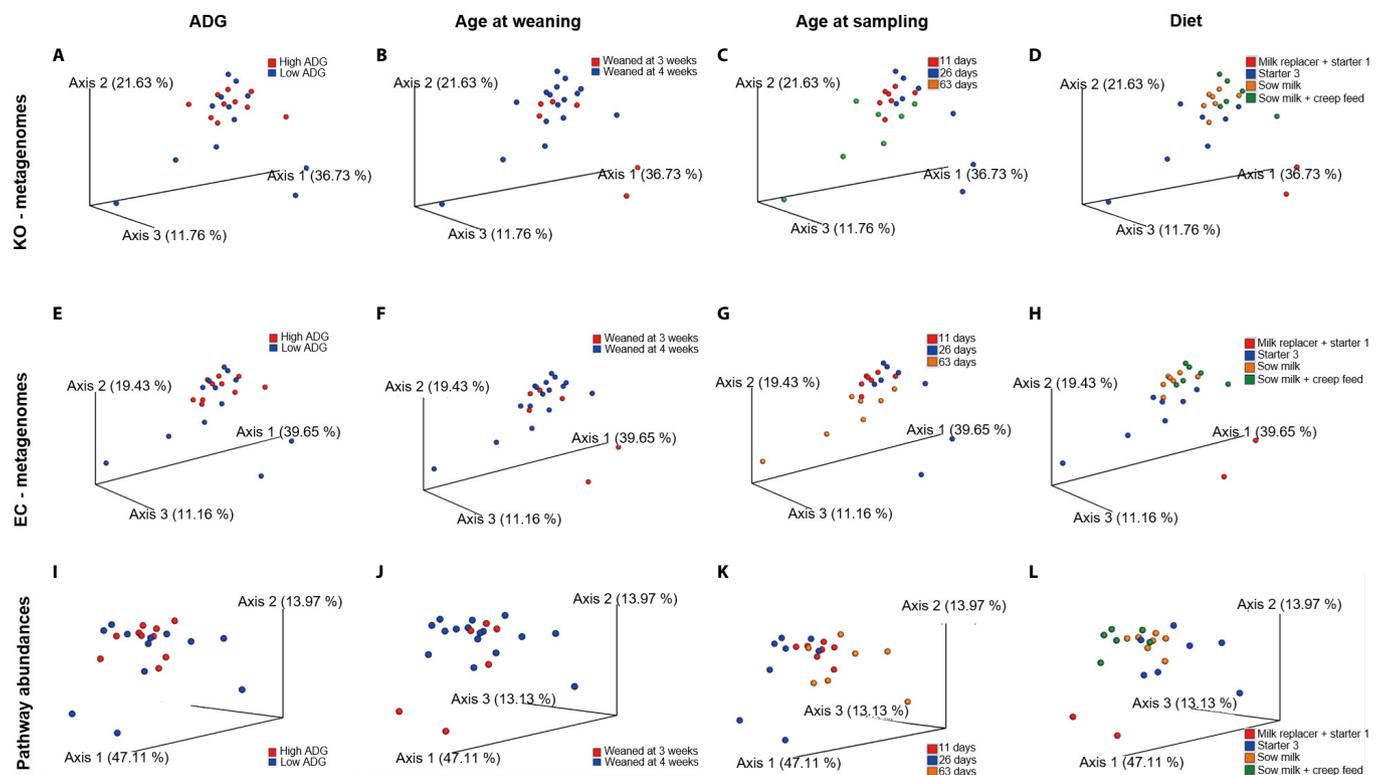

Fig. S2. Principle Coordinate Analysis (PCoA) plots using Bray Curtis distances to show the distribution of oropharyngeal microbiomes in samples collected at 11, 26 and 63 days of age. In (A–D) is the distribution based on the predicted KEGG Orthology (KO) metagenomes; in (E–H), the distribution based on predicted enzymes; and in (I–L) the distribution based on the predicted pathway abundances. The symbols represent data from individual piglets, color-coded by the indicated categories of metadata.